

# Composition of adipose tissue and marrow fat in humans by $^1\text{H}$ NMR at 7 Tesla

Jimin Ren,<sup>\*,†</sup> Ivan Dimitrov,<sup>\*,§§</sup> A. Dean Sherry,<sup>\*,†,\*\*</sup> and Craig R. Malloy<sup>1,\*,†,§,††</sup>

Advanced Imaging Research Center,<sup>\*</sup> Department of Radiology,<sup>†</sup> and Department of Internal Medicine,<sup>§</sup> University of Texas Southwestern Medical Center, Dallas, TX 75235; Department of Chemistry,<sup>\*\*</sup> University of Texas at Dallas, Richardson, TX 75083; Veterans Administration North Texas Health Care System,<sup>††</sup> Dallas, TX 75216; and Philips Medical Systems,<sup>§§</sup> Cleveland, OH 44143

**Abstract** Proton NMR spectroscopy at 7 Tesla (7T) was evaluated as a new method to quantify human fat composition noninvasively. In validation experiments, the composition of a known mixture of triolein, tristearin, and trilinolein agreed well with measurements by  $^1\text{H}$  NMR spectroscopy. Triglycerides in calf subcutaneous tissue and tibial bone marrow were examined in 20 healthy subjects by  $^1\text{H}$  spectroscopy. Ten well-resolved proton resonances from triglycerides were detected using stimulated echo acquisition mode sequence and small voxel ( $\sim 0.1$  ml), and  $T_1$  and  $T_2$  were measured. Triglyceride composition was not different between calf subcutaneous adipose tissue and tibial marrow for a given subject, and its variation among subjects, as a result of diet and genetic differences, fell in a narrow range. After correction for differential relaxation effects, the marrow fat composition was  $29.1 \pm 3.5\%$  saturated,  $46.4 \pm 4.8\%$  monounsaturated, and  $24.5 \pm 3.1\%$  diunsaturated, compared with adipose fat composition,  $27.1 \pm 4.2\%$  saturated,  $49.6 \pm 5.7\%$  monounsaturated, and  $23.4 \pm 3.9\%$  diunsaturated. **■** Proton spectroscopy at 7T offers a simple, fast, noninvasive, and painless method for obtaining detailed information about lipid composition in humans, and the sensitivity and resolution of the method may facilitate longitudinal monitoring of changes in lipid composition in response to diet, exercise, and disease.—Ren, J., I. Dimitrov, A. D. Sherry, and C. R. Malloy. Composition of adipose tissue and marrow fat in humans by  $^1\text{H}$  NMR at 7 Tesla. *J. Lipid Res.* 2008. 49: 2055–2062.

**Supplementary key words** fatty acids • triglycerides • spectroscopy • metabolism • bone marrow • subcutaneous fat • musculoskeletal • lipid composition • in vivo

Adipose mass and the anatomic distribution of adipose tissue strongly influence the risk of multiple diseases. The fatty acid composition of adipose tissue may also influence predisposition to various disorders including cancer (1, 2), type 2 diabetes (3–6), and heart disease (7). Nevertheless,

the relations among adipose tissue composition and the risk of disease are controversial and difficult to study, in part because of the traditional requirement for invasive biopsy. Noninvasive analysis of fat composition in humans by  $^1\text{H}$  NMR spectroscopy would have major advantages, because the study could be integrated into routine exams. Under high-resolution analytical conditions, signals from protons adjacent to double bonds are easily resolved, and it is a relatively simple matter to assess fat composition by  $^1\text{H}$  NMR spectroscopy (8–12). However, extension of these methods to human applications is challenging because chemical shift resolution observed in vivo at 1.5 or 3.0 Tesla (T) is substantially worse than in analytical spectrometers. Because of the intense current interest in triglyceride composition and metabolism, several alternatives have been suggested, including selective detection of polyunsaturated fatty acids in animal models at 4.7 T (13), two-dimensional NMR at 3 T (14), and  $^1\text{H}$ -decoupled  $^{13}\text{C}$  NMR spectroscopy (15–19). The large chemical shift dispersion of  $^{13}\text{C}$  is a major advantage compared with  $^1\text{H}$  observations. Wide application, however, is limited by the requirement for additional coils and a second radiofrequency channel.

Chemical shift resolution in the  $^1\text{H}$  spectrum should, in principle, improve at higher fields. Recently, the fatty acid composition of mouse adipose tissue was reported based on  $^1\text{H}$  spectra obtained in vivo at 7T, where the chemical shift dispersion allows assignment of signals from protons adjacent to double bonds. One advantage of this analysis (20) was the use of spectroscopic data from three adjacent resonances with a frequency bandwidth (BW) of only 0.74 ppm (221 Hz at 7T). In other reports (8), triglyceride saturation was determined from the olefinic protons ( $-\text{CH}=\text{CH}-$ , at  $\sim 5.31$  ppm) by using the  $\text{CH}_3$  methyl protons (at  $\sim 0.90$  ppm) as the reference. These two reso-

This study was supported by the National Institutes of Health (Grant RR-02584) and the Department of Defense (Contract number W81XWH-06-2-0046).

\* Author's Choice—Final version full access.

Manuscript received 8 February 2008 and in revised form 27 May 2008.

Published, JLR Papers in Press, May 28, 2008.  
DOI 10.1194/jlr.D800010-JLR200

Abbreviations: BW, bandwidth; MRS, magnetic resonance spectroscopy; NA, number of acquisitions; NP, number of points; PRESS, point-resolved spectroscopy; STEAM, stimulated echo acquisition mode; 7T, 7 Tesla; TE, echo time; TR, repetition time.

<sup>1</sup>To whom correspondence should be addressed.  
e-mail: Craig.Malloy@UTSouthwestern.edu

nances span a frequency range of 4.41 ppm (1,314 Hz at 7T). The wide BW may result in less-uniform excitation profiles, and the use of frequency-dependent spatial localization yields spectra with resonances originating in different physical locations, an artifact known as chemical shift displacement.

The ability to noninvasively monitor triglyceride composition using proton spectroscopy would have wide applications in clinical research. In this study, the approach described by Strobel, van den Hoff, and Pietzsch (20) to measuring fatty acid composition by  $^1\text{H}$  NMR spectroscopy in mice was tested in phantoms and extended to healthy human subjects. The fatty acid composition of bone marrow measured by NMR in this study was in good agreement with some (12) but not all (21) reports of fatty acid composition by gas chromatography. The NMR determination of saturated fatty acids in extremity subcutaneous fat agreed well with gas chromatographic analysis of abdominal subcutaneous fat, about 27% of fatty acids. Somewhat lower values for monounsaturated fats, about 50%, were found by NMR, compared with 57% found in biopsy studies. The principles used by numerous investigators to quantify fat composition by  $^1\text{H}$  NMR (8–12, 20) are easily extended to human studies at 7T, where high-quality  $^1\text{H}$  NMR spectra can be obtained routinely.

## MATERIALS AND METHODS

### Human MR spectroscopy

The protocol was approved by the Institutional Review Board. Informed consent was obtained from all participants prior to the study. Twenty healthy adults (twelve females and eight males) age 22–52 years (average 34 years; without diabetes or known vascular disease) were studied supine or prone in a 7T system (Achieva, Philips Medical Systems, Cleveland, OH). Spectra were acquired with a partial-volume quadrature transmit/receive coil customized to fit the shape of a human calf. Axial, coronal, and sagittal  $T_2$ -weighted turbo spin echo images were initially acquired of the left calf muscle. Typical parameters were: field of view  $180 \times 180$  mm, repetition time (TR) 1,500 ms, echo time (TE) 75 ms, turbo factor 16, and number of acquisitions (NA), 1. Single-voxel stimulated echo acquisition mode (STEAM) (typical parameters: voxel size  $5 \times 5 \times 5$  mm<sup>3</sup> ( $\sim 0.1$  ml), TR 2,000 ms, TE 20 ms, spectral BW of 4 kHz, number of points (NP) 4,096 and zero-filled to 8,192 prior to Fourier transform, NA 16, no water suppression) was used to acquire  $^1\text{H}$  spectra from tibial bone marrow and subcutaneous fat tissue. To correct individual resonances for relaxation effects,  $T_1$  and  $T_2$  were measured in seven of the subjects.  $T_1$  was measured using inversion-recovery, with nine inversion delay times in the range of 5 ms to 3,000 ms, with TR 7 s and TE 40 ms.  $T_2$  was measured by using ten TE values from 20 ms to 180 ms, with TR 8 s. Subjects were instructed to move slowly in the scan room. The entire scanning session was 60 min or less and it was well-tolerated by all subjects. All subjects were interviewed after the exam and again at 24 h after the exam. All subjects specifically denied dizziness, nausea, vertigo, headaches, or visual changes.

### Phantom studies

Pure triacylglycerols were obtained from Nu-Chek Prep, Inc. (Elysian, MN). To test the accuracy of the protocol to quantify

lipid composition, phantom samples were prepared by mixing tristearin (18:0) (number of carbons:number of double bonds), triolein (18:1), and trilinolein (18:2) in the following ratios: 50:0:50, 50:10:40, 50:20:30, 50:30:20, 50:40:10, 50:50:0, and 25:50:25. Phantom samples with composition of different chain lengths of triglyceride were prepared by mixing tripalmitin (16:0) and tristearin (18:0) in the following ratios: 100:0, 80:20, 75:25, 50:50, 25:75, 20:80 and 0:100. All mixtures were dissolved in  $\text{CD}_3\text{Cl}$  in 4 ml glass vials, which were then mounted in the center of a 150 ml beaker filled with deionized water. Typical magnetic resonance spectroscopy (MRS) parameters were: TR 8 s, TE 11 ms, voxel size 0.2 ml, NP 16 k, BW 8 kHz, NA 128. The triglyceride composition was calculated as described below.

### Spectral analysis

The  $^1\text{H}$  chemical shift of in vivo fat resonances from bone marrow and subcutaneous tissue was assigned such that the methyl signal was at 0.9 ppm. Resonance areas were determined by fitting the spectra with Voigt shapes (variable proportions of Lorentzian plus Gaussian) on ACD software (Advanced Chemistry Development, Inc., Toronto, Canada) after phasing and baseline correction. Peak areas for each individual resonance were corrected with its corresponding  $T_1$  and  $T_2$ . Lipid composition was evaluated after correction for relaxation effects.

### Calculation of triglyceride composition

Human adipose tissue is composed largely of triglycerides. Seven fatty acids predominate as follows (number of carbons: number of double bonds, typical abundance): myristic (14:0, 3%), palmitic (16:0, 19–24%), palmitoleic (16:1, 6–7%), stearic (18:0, 3–6%), oleic (18:1, 45–50%), linoleic (18:2, 13–15%), and linolenic (18:3, 1–2%) (22, 23). These fatty acids account for well over 90% of the fatty acids in human adipose tissue. Odd-carbon fatty acids, longer chain fatty acids, and shorter chain fatty acids account for the remainder. Each of these less-abundant fats individually contributes much less than 1% (22).

At 7 T, 10 resonances can be resolved, designated here as A to J in alphabetic order from upfield to downfield (Fig. 1). Six resonances contribute equivalent information about triglyceride composition: the  $\text{CH}_3$  methyl protons (labeled A, at  $\sim 0.90$  ppm), the  $\text{CH}_2$  methylene protons  $\alpha$ - (E, at  $\sim 2.25$  ppm) and  $\beta$ - (C, at  $\sim 1.59$  ppm) to the carbonyl, and the glycerol backbone CH (I) and  $\text{CH}_2$  protons (G and H). Hence, there are only four additional informative resonances to consider: 1) bulk  $\text{CH}_2$  methylene protons (labeled B at  $\sim 1.3$  ppm); 2) allylic  $\text{CH}_2$  protons,  $\alpha$ - to a double bond, at 2.03 ppm (D); 3) diallylic (also called bis-allylic)  $\text{CH}_2$  protons at 2.77 ppm (F); and 4) olefinic, double bond  $-\text{CH}=\text{CH}-$  protons at 5.31 ppm (J), which partially overlap with the glycerol CH methine proton at 5.21 ppm (I).

It was assumed that the fatty acids detected here contain either 0, 1, or 2 double bonds. These three types of fatty acids account for  $\sim 97$ – $98\%$  of total fat in humans on ordinary Western diets. Linolenic acid (18:3) is excluded in this simplification, but it contributes only  $\sim 0.5\%$  of the total triglycerides (22). With this assumption,  $f_{\text{sat}} + f_{\text{mono}} + f_{\text{di}} = 1$  where  $f_{\text{sat}}$ ,  $f_{\text{mono}}$ , and  $f_{\text{di}}$  refer to the fraction of fatty acids that are saturated, monounsaturated, and doubly unsaturated (or diunsaturated), respectively. The fraction that is diunsaturated,  $f_{\text{di}}$ , can be determined directly from the relative area of the resonance of the “bridging” diallylic protons (resonance F), with respect to the resonance of methylene protons  $\alpha$  to COO (resonance E):

$$f_{\text{di}} = \text{area (F/E)} \quad (\text{Eq. 1})$$

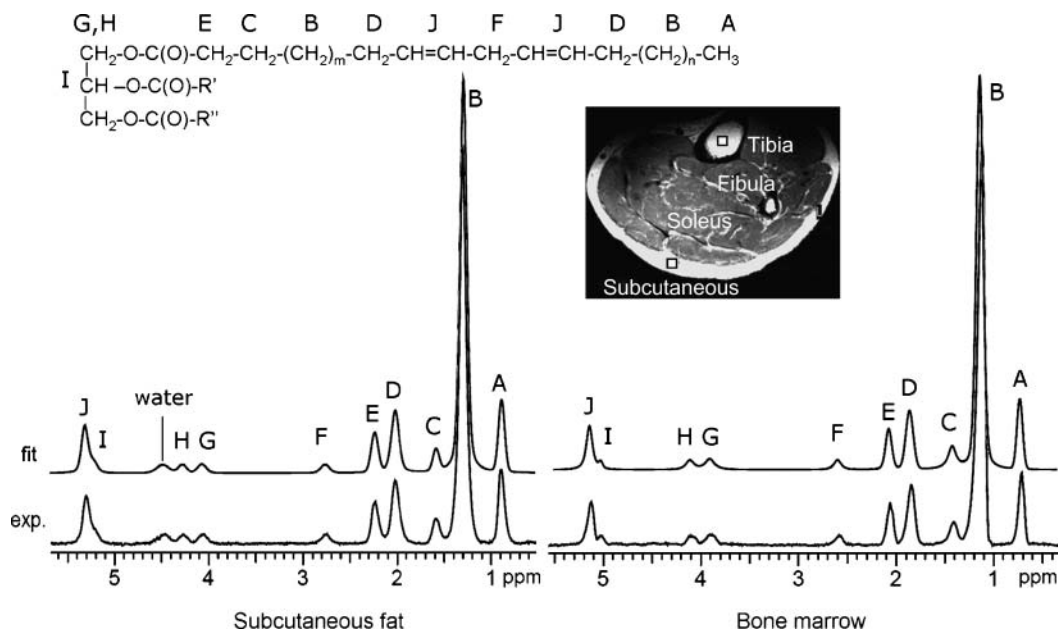


**Fig. 1.**  $^1\text{H}$  NMR spectra of subcutaneous fat (left) and tibial bone marrow (right) from a 26 year-old healthy male at 7 Tesla (7T). Ten resonances can be resolved (A–J). The bottom trace shows the acquired spectrum, and the upper trace shows the fitted spectrum. A water signal is seen in the spectrum of subcutaneous fat but not bone marrow. A  $T_2$ -weighted image shows the position of the voxel in the subcutaneous fat tissue and tibial bone marrow ( $5 \times 5 \times 5 \text{ mm}^3$ ) from which the spectra were acquired.

Once the  $f_{\text{di}}$  value is determined, one can evaluate  $f_{\text{mono}}$  from the relative area of proton resonance  $\alpha$  to the double bond by:

$$f_{\text{mono}} = 0.5 * \text{area} (D/E) - f_{\text{di}} \quad (\text{Eq. 2})$$

The remaining unknown  $f_{\text{sat}}$ , the fraction of saturated fatty acid, is derived as  $f_{\text{sat}} = 1 - (f_{\text{mono}} + f_{\text{di}})$ .

Assuming that  $f_{16\text{C}} + f_{18\text{C}} = 1$ , the fraction of fatty acids that are 16 carbon versus 18 carbon can be determined from the area of the bulk methylene resonances  $(-\text{CH}_2)_n$ :

$$\text{Area} (B/E) = f_{16\text{C}}(12f_{\text{sat}} + 8f_{\text{mono}}) + f_{18\text{C}}(14f_{\text{sat}} + 10f_{\text{mono}} + 7f_{\text{di}}) \quad (\text{Eq. 3})$$

The coefficients in front of the individual fractions are: 12 for palmitic acid (16:0), 8 for palmitoleic acid (16:1), 14 for stearic acid (18:0), 10 for oleic acid (18:1), and 7 for linoleic acid (18:2). This analysis is essentially identical to the earlier analysis (20) with the exception that a term for an unsaturated fat with three double bonds was omitted rather than assuming a low, fixed concentration.

## RESULTS

Ten lipid resonances are typically observed in the 7T  $^1\text{H}$  spectrum from physiological fats (Fig. 1). Except for the double-bond protons, which partially overlap the methine proton of the glycerol backbone (the chemical shift difference is about 0.1 ppm), the lipid resonances were well-resolved at 7T and qualitatively similar to high-resolution spectra obtained in mice (20). The water signal generally appears in the  $^1\text{H}$  spectrum of subcutaneous fat tissue, with subject-dependent intensity and line width, but it is

nearly undetectable in bone marrow acquired from a small voxel ( $\sim 0.1 \text{ ml}$ ). The resonance assignments, chemical shifts, and relative intensities from both marrow and subcutaneous fat are summarized in **Table 1**.

The validity of this analysis was tested by mixing three  $\text{C}_{18}$  triacylglycerols and, in a separate experiment, by mixing  $\text{C}_{16}$  and  $\text{C}_{18}$  triacylglycerols, in various ratios. **Figure 2A** shows data collected from phantoms, with the area (F/E) plotted against the actual known fraction of trilinolein ( $f_{\text{di}}$ ) in the  $\text{C}_{18}$  mixture phantom samples. A linear correlation is seen between the measured F/E ratio and the sample true  $f_{\text{di}}$  value, with linear coefficient of 1.02 and correlation coefficient  $R^2 = 0.992$ . Similar correlations were found for the other components (data not shown). **Figure 2B** shows the measured  $\text{C}_{18}$  triacylglycerol fraction ( $f_{18\text{C}}$ ) against the actual known  $\text{C}_{18}$  fraction in the  $\text{C}_{16}$  and  $\text{C}_{18}$  mixture phantom samples. The plot of the known  $f_{18\text{C}}$  versus the measured  $f_{18\text{C}}$ , which was evaluated by  $0.5 * \text{area} (B/E) - 12$ , also yielded a linear dependence, with linear coefficient of 0.94 and correlation coefficient  $R^2 = 0.992$ .

For quantitation of fat composition in human subcutaneous tissue and tibial marrow, the signal intensities were corrected for all differences in  $T_1$  and  $T_2$  as determined from inversion-recovery (**Fig. 3**) and TE-dependent (**Fig. 4**) experiments, respectively. **Figure 3** shows the  $T_1$  (left) and  $T_2$  (right) spectra collected from the same voxel located in subcutaneous tissue, together with the corresponding curve fittings (bottom). **Figure 4** compares the  $T_2$  data between tibial marrow and subcutaneous tissue collected from same-sized voxels, on the same volunteer. The measured  $T_1$  and  $T_2$  values at this field are summa-

TABLE 1. Chemical shifts and relative resonance areas

Letter and Structure	Chemical Group	Chemical Shift <i>ppm</i>	Resonance Areas	
			Marrow	Subcutaneous
A (methyl protons)	-CH <sub>3</sub>	0.90	130.2 ± 11.3	125.8 ± 14.5
B (methylene protons)	-(CH <sub>2</sub> ) <sub>n</sub> -	1.30	935.0 ± 59.2	956.4 ± 73.1
C (methylene protons β to COO)	-CH <sub>2</sub> -CH <sub>2</sub> -COO	1.59	104.5 ± 12.3	109.1 ± 15.4
D (methylene protons α to C = C)	-CH <sub>2</sub> -CH = CH-CH <sub>2</sub> -	2.03	141.7 ± 10.8	146.0 ± 15.2
E (methylene protons α to COO)	-CH <sub>2</sub> -COO	2.25	100	100
F (diallylic methylene protons)	=CH-CH <sub>2</sub> -CH =	2.77	24.5 ± 3.1	23.4 ± 3.9
J (methine protons)	-CH = CH-	5.31	62.4 ± 5.7	63.9 ± 6.2

The areas are relative to the methylene resonance α to COO (peak E) after correction for partial saturation. Resonance assignments by letter correspond to Fig. 1. Values are the mean ± 1 SD (n = 20).

rized in **Table 2**. As shown by the data, protons at different structural positions in fats have quite different values, with T<sub>1</sub>s ranging from 0.32–1.16 s, and T<sub>2</sub>s ranging from 30–74 ms. Calf subcutaneous fat has shorter T<sub>1</sub> and T<sub>2</sub> values, about 7% on average, in comparison with tibial bone marrow. It should be pointed out that because of the presence of proton J-coupling, these T<sub>1</sub> and T<sub>2</sub> values are valid only for STEAM sequence. Shorter T<sub>2</sub> values have been reported for animal abdominal fat using point-resolved spectroscopy (PRESS) sequence (20) at the same field strength.

The derived fractions of saturated, monounsaturated and diunsaturated fat constituents are summarized in **Table 3**, together with the estimated fraction of fatty acid chain length f<sub>16C</sub> and f<sub>18C</sub>. The composition of bone marrow and adipose fat was not significantly different, with an average 29.1 ± 3.5% saturated, 46.4 ± 4.8% monounsaturated, and 24.5 ± 3.1% diunsaturated fractions for marrow, as compared with 27.1 ± 4.2% saturated, 49.6 ± 5.7% monounsaturated, and 23.4 ± 3.9% diunsaturated fractions for subcutaneous fat. A good linear correlation

was seen between tibial marrow and subcutaneous fat in the measured area ratio (F/E), which is the index of diunsaturated fraction, for the 20 subjects studied, as shown in **Fig. 5**. In addition, a composition of 33.4 ± 4.9% from fatty acid with 16 carbons and 66.5 ± 9.7% from fatty acid with 18 carbons was calculated for bone marrow, as compared with subcutaneous fat with a composition of 23.4 ± 3.9% for 16 carbon fraction and 73.8 ± 17.8% for 18 carbon fraction.

## DISCUSSION

High-quality <sup>1</sup>H NMR spectra from human adipose tissue were obtained routinely at 7T. The features of the <sup>1</sup>H spectra at 7T were consistent with spectra of triacylglycerols obtained under high-resolution conditions (8–12) or in mice at 7T (20). Perhaps the most significant observation was that chemical shift dispersion in humans is greatly improved compared with 1.5 T or 3.0 T. The ability to resolve protons adjacent to double bonds allows non-

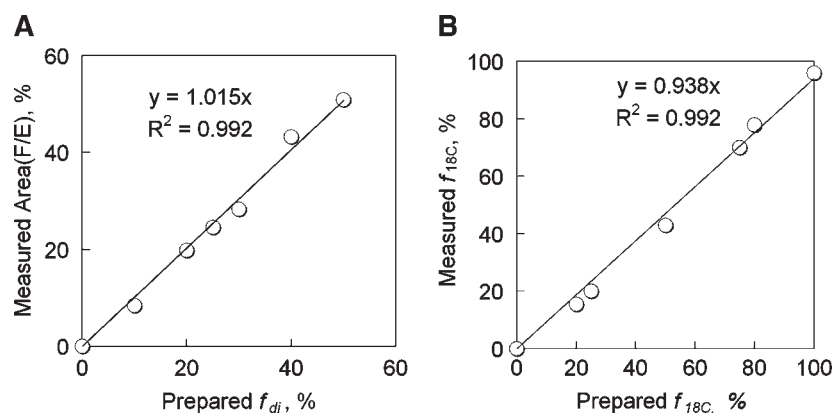


**Fig. 2.** A: Correlation of the known, prepared fraction of diunsaturated triglyceride with MR-measured fraction of diunsaturated triglyceride. Phantoms were prepared by mixing three C18 triglycerides (number of double bonds), tristearin (0), triolein (1), and trilinolein (2) in the following ratios (tristearin:triolein:trilinolein): 50:0:50, 50:10:40, 50:20:30, 50:30:20, 50:40:10, 50:50:0, and 25:50:25. <sup>1</sup>H NMR spectra of the phantoms were analyzed using Equations 1 and 2. B: Correlation of the known, prepared fraction of C18 triglyceride with MR-measured value from area (B/E). Phantoms were prepared by mixing C16 tripalmitin and C18 tristearin with the following ratios (C16:C18): 100:0, 80:20, 75:25, 50:50, 25:75, 20:80, and 0:100. The data were analyzed using  $f_{18C} = 0.5 \cdot \text{area (B/E)} - 12$ .

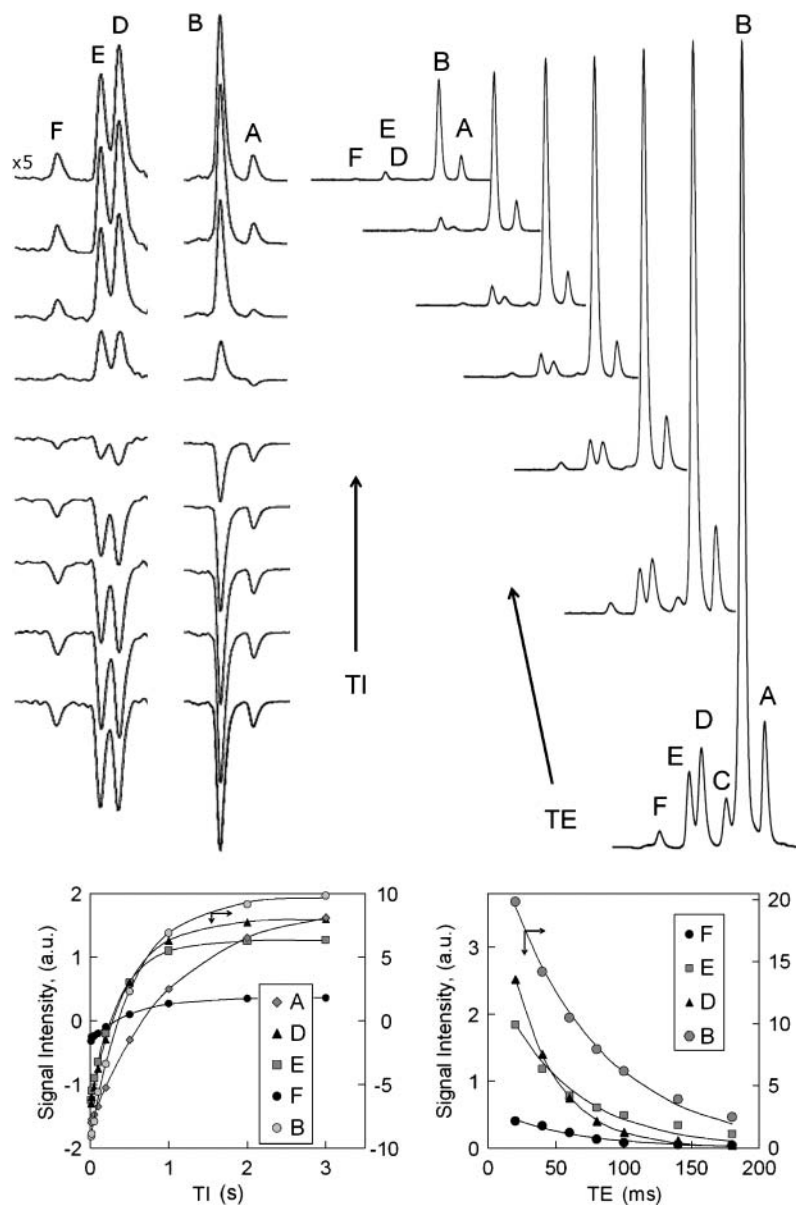


**Fig. 3.** Inversion-recovery measurement of  $T_1$  (left panel) and echo time (TE)-dependence measurement of  $T_2$  (right panel) from subcutaneous fat tissues of a 34 year-old healthy male at 7T. The inversion bandwidth (BW) was set to span resonances A and B (middle stack), or resonances C, D, E, and F (left-most stack). The inversion delay times for the given spectra are 10, 20, 50, 100, 200, 500, 1,000, 2,000, and 3,000 ms with a constant repetition time (TR) of 7 s and TE of 40 ms (left panel). The echo times for the  $T_2$  measurements are 20, 40, 60, 80, 100, 140, and 180 ms (right panel).

invasive estimation of the fatty acid composition of adipose tissue.

Proton-decoupled  $^{13}\text{C}$  NMR of human adipose tissue (15–19) allows more-detailed characterization of fat composition, compared with a  $^1\text{H}$  spectrum. For example, the outer unsaturated carbons in a bisallylic group ( $-\text{CH}_2-\text{CH}=\text{CH}-\text{CH}_2-\text{CH}=\text{CH}-\text{CH}_2-$ ) are resolved from the inner carbons in spectra obtained in vivo at 1.5 T. Natural abundance  $^{13}\text{C}$  NMR is limited by relatively low sensitivity, low spatial resolution and additional technical requirements, all disadvantages compared with  $^1\text{H}$  spectroscopy for human study. Conversely, 7T instruments are not widely available. However, because the number of 7T instruments in medical sites is increasing steadily and  $^1\text{H}$  spectroscopy is routine on all systems, it seems reasonable to anticipate use of  $^1\text{H}$  spectroscopy at 7T for clinical research.

At 7T, ten proton resonances in the chemical shift span of 0.9–5.3 ppm are resolved. The three resonances in the narrow range of 2.03–2.77 ppm provide an internal standard plus information about the abundance of protons between or adjacent to double bonds. This information, after correction for relaxation, allows calculation of the relative concentration of saturated, monounsaturated, and diunsaturated fatty acids. The proposed analysis of lipid composition was confirmed by comparison to authentic standards.

The fraction of saturated fats in triglycerides as determined by  $^1\text{H}$  NMR spectroscopy at 7T, about 27–29%, is in excellent agreement with literature values. However, the fraction of fatty acids that are monounsaturated was somewhat less (about 46–50%) in this study, compared with biopsy studies, where about 55–60% monounsaturated fatty acids are typically found (22, 24). Consequently,

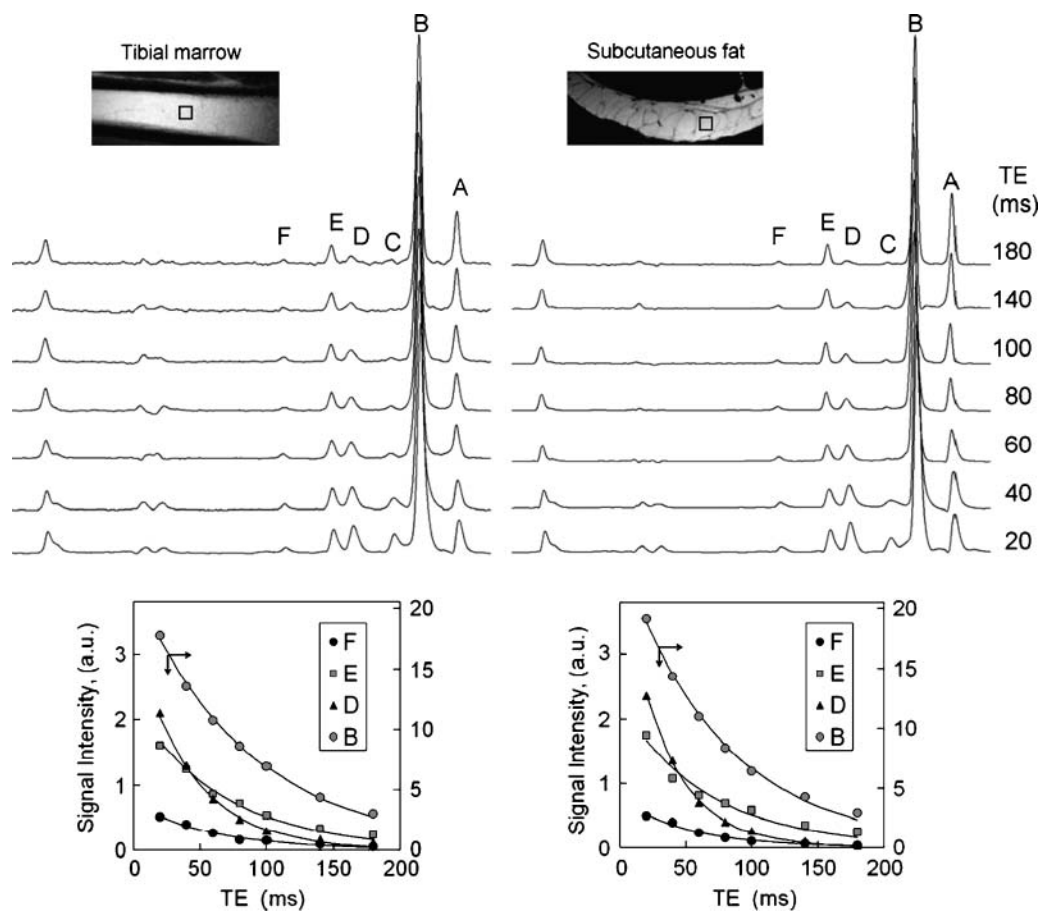


**Fig. 4.**  $T_2$  measurement of tibia bone marrow (left panel) and calf subcutaneous fat (right panel) from a 25 year-old healthy female by varying TEs at 7T. Note that the voxel ( $5 \times 5 \times 5 \text{ mm}^3$ ) fits well in the single fat cell of the subcutaneous tissue and the collected  $^1\text{H}$  spectrum is water-free. All spectra are vertically scaled to equal magnitude of the methylene resonance (B), and as a result, with TE increase, the methyl resonance A with longer  $T_2$  than B shows signal rising, whereas the shorter  $T_2$  resonances such as C and D show signal decaying relative to resonance B. To avoid overcrowding, the fitting of the “A” and “C” peaks is not shown. Other parameters: TR 8 s, number of acquisitions, 8; number of points, 4 k; BW 4 kHz.

the fraction of fatty acids estimated to be diunsaturated was about 23–24% in this study compared with about 17–18% in biopsy studies.

At least three technical issues may contribute error in this analysis. First, macromolecules or aqueous metabolites with chemical shifts overlapping the lipid resonances may alter the estimates of relative intensity. Second, the signals *in vivo* are the sum of very complex  $^1\text{H}$  spin-coupled multiplets from several different fatty acids with

slightly different chemical shifts. Consequently, a single Lorentzian-Gaussian line does not properly represent the observed lineshape. Even when high-resolution analytical  $^1\text{H}$  NMR was used to measure marrow fat composition from samples extracted in chloroform, thereby removing aqueous species and other complicating factors that may contribute error in the study of intact tissue, the NMR method overestimated the fraction of saturated fatty acids, compared with “gold standard” gas chromatography of the

TABLE 2. Relaxation times in resonances assigned to the fatty acid chain ( $n = 3-6$ )

Chemical Group	$T_1$ , Second ( $n = 3$ )		$T_2$ , Milliseconds ( $n = 6$ )	
	Marrow	Subcutaneous	Marrow	Subcutaneous
$-\text{CH}_3$ (A)	$1.16 \pm 0.04$	$1.08 \pm 0.05$	$74 \pm 6$	$67 \pm 8$
$-(\text{CH}_2)_{n-1}$ (B)	$0.55 \pm 0.03$	$0.53 \pm 0.04$	$69 \pm 4$	$63 \pm 5$
$-\text{CH}_2-\text{CH}_2-\text{COO}$ (C)	$0.39 \pm 0.04$	$0.32 \pm 0.05$	$33 \pm 6$	$30 \pm 6$
$-\text{CH}_2-\text{CH} = \text{CH}-\text{CH}_2-$ (D)	$0.42 \pm 0.02$	$0.39 \pm 0.03$	$42 \pm 2$	$39 \pm 3$
$-\text{CH}_2-\text{COO}$ (E)	$0.44 \pm 0.02$	$0.40 \pm 0.02$	$60 \pm 3$	$55 \pm 4$
$=\text{CH}-\text{CH}_2-\text{CH} =$ (F)	$0.60 \pm 0.03$	$0.58 \pm 0.03$	$59 \pm 3$	$58 \pm 3$

The values shown are mean  $\pm$  SD and are valid for the stimulated echo acquisition mode pulse sequence used.

TABLE 3. Average fat composition in marrow and subcutaneous tissues

	Marrow	Subcutaneous
Relative concentration		
Saturated ( $f_{\text{sat}}$ )	29.1 $\pm$ 3.5	27.1 $\pm$ 4.2
Monounsaturated ( $f_{\text{mono}}$ )	46.4 $\pm$ 4.8	49.6 $\pm$ 5.7
Diunsaturated ( $f_{\text{di}}$ )	24.5 $\pm$ 3.1	23.4 $\pm$ 3.9
Chain length		
Fraction 16-carbon ( $f_{16\text{C}}$ )	33.5 $\pm$ 4.9	26.2 $\pm$ 6.4
Fraction 18-carbon ( $f_{18\text{C}}$ )	66.5 $\pm$ 9.7	73.8 $\pm$ 17.9

The relative concentration, as percentage of saturated, monounsaturated, and diunsaturated fats, as well as the fraction of 16- vs. 18-carbon fats are shown. Values are the mean  $\pm$  1 SD ( $n = 20$ ).

same samples (12). Third, as emphasized earlier (20), correction for  $T_2$  is also essential and more important than correction for  $T_1$  differences. For a typical TE of 11 ms, the relative difference in  $T_2$  correction among the resonances D, E, and F accounts for  $\sim 4\%$ , but it reaches 8% at TE = 20 ms, and is as large as 18% at TE = 40 ms. This compares to only about 1% difference after correction for  $T_1$  effects for the same three resonances at TR = 2 s. The  $T_1$  correction is not needed when the spectrum is collected with TR of 4 s. It is found that the calf subcutaneous fat has relatively shorter ( $\sim 7\%$ ) proton relaxation times than the marrow (Table 2), indicating a larger local Bo field inhomogeneity on subcutaneous tissue. This can be understood from the difference in the microscopic structure between these two types of adipose tissues, as shown in the MRI images (Fig. 4, insert), in which subcutaneous tissue is seen as packed with large fat cells of different sizes, embedded with rich vasculature, and curvedly shaped, whereas the bone marrow appears as fine uniform structure, aligned straight inside the tibial bone, and nearly parallel to the Bo field. Because of this, the spectral resolution from bone marrow is generally superior to that from subcutaneous fat, as shown in Fig. 1.

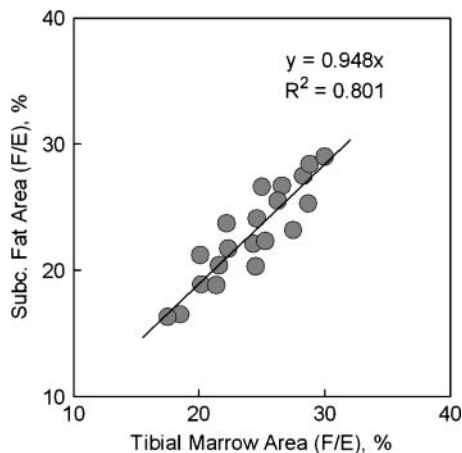


Fig. 5. Correlation of measured area (F/E) between tibial bone marrow and subcutaneous fat for the 20 healthy adult subjects studied, showing that the diunsaturated fatty acid is similar for these two adipose sites and that the fat composition variation among subjects is detectable by  $^1\text{H}$  magnetic resonance spectroscopy.


It is probably unrealistic to anticipate perfect correlation between this MR analysis of extremity fat and marrow compared with literature data obtained largely from the abdomen, chest, or buttocks. There are complex effects of diet, season, gender, and anatomical site on fatty acid composition (24, 25). For example, extremity adipose tissue has a greater fraction of monounsaturated fat and less saturated fat compared with subcutaneous fat from the chest and abdomen (25). These factors were not controlled in the current study. Nevertheless, the average ratio  $f_{\text{di}}/f_{\text{mono}}$  (47% for subcutaneous fat and 53% for bone marrow, Table 3) obtained from this  $^1\text{H}$  MRS study for 20 adult subjects (average age 34), is in excellent agreement with a previously reported value (50%) for the ratio of polyunsaturated to monounsaturated fatty acid by in vivo  $^{13}\text{C}$  study (19) of calf subcutaneous tissue of 17 adult subjects (average age 30). The obvious advantage of  $^1\text{H}$  MRS is that it is fast (less than 1 min), has a low specific absorption rate (no need for broadband decoupling as in  $^{13}\text{C}$ ), is easily localized (not a volume detection), and is typically more easily implemented (no special scanner hardware or coil required). The high resolution and sensitivity of the current STEAM-based  $^1\text{H}$  MR analysis also enable the detection of fat composition variation among uncontrolled healthy subjects (Fig. 5), which might be attributed to the difference in individuals' long-term diet and metabolic genetics. Therefore, it is anticipated that the method may be useful in rapid detection of substantial changes in the composition of fatty acids in response to diet, exercise, and fat-metabolic diseases. This method, in our view, would help advance noninvasive human lipid research, which has been focused on studying fat mass distribution by MRI and other techniques rather than fat molecular structural composition. In addition, an analysis of our data (not shown) indicates no obvious difference in fat composition between male and female subjects, although, on average, the calf subcutaneous fat in female is approximately two-fold thicker than in male.

The decision to simplify the description of fatty acid composition to saturated, monounsaturated, and diunsaturated fats was based on two considerations. First, the amount of polyunsaturated fats (three or more double bonds) in human adipose tissue contributes very little, less than 1–2%, to the total  $^1\text{H}$  NMR signal. Second, earlier studies that were able to quantify triply unsaturated fatty acids separate from other fatty acids required high-resolution analytical conditions (10–12). For practical purposes in humans, this achievement would mean the capacity to separately quantify oleic (18:1), linoleic (18:2), and linolenic (18:3) acid. However, at the resolution achieved in these studies, a 50:50 mixture of triolein:trilinolenin is indistinguishable from a spectrum of trilinolein. For these reasons, the description of fatty acids as saturated, monounsaturated, or diunsaturated seems a reasonable simplification.

Frequency-dependent spatial localization introduces a chemical shift displacement artifact in the  $^1\text{H}$  MR spectrum. Quantitation may be inaccurate if it is based on ratios of two resonances when the region of interest is close to the inter-tissue boundary. Although this effect was not

critically evaluated in this study, the use of a small voxel (~0.1 ml) well within the bone marrow plus analysis of resonances over a narrow chemical shift range reduces susceptibility to chemical shift displacement effects. Unlike the methyl resonance, the resonance of protons  $\alpha$  to the carbonyl is not affected by the neighboring large bulk  $\text{CH}_2$  (resonance B), which often induces an uneven baseline at nearby resonances at shorter TEs. Although this baseline problem can be improved at longer TEs, the faster decay of protons  $\alpha$  to a double bond (resonance D,  $T_2 = 42$  ms for marrow, and 39 for subcutaneous fat) than the reference resonance E ( $T_2 = 59$  ms) makes long TE scan conditions less favorable. STEAM sequence has the advantage of shorter TE than PRESS and less dependence on proton J modulation due to the smaller TE/ $T_2$  ratio, and therefore was chosen for the quantification of fat composition in this method.

In addition to composition analysis, the well-resolved resonances of human tibial bone marrow and calf subcutaneous fat at 7T could also be very useful as an internal standard to quantify intramuscular lipids (26), which have attracted great research interest over the last few years, owing to their relation to insulin sensitivity, diabetes, and obesity (27).

In conclusion, this  $^1\text{H}$  MRS study at 7T indicates that the rapid acquisition of high-quality  $^1\text{H}$  NMR spectra from subcutaneous fat and from bone marrow is straightforward in healthy volunteers, and that the spectra may be analyzed to assess triglyceride composition. This may facilitate longitudinal monitoring of changes in lipid composition in response to diet, exercise, and disease. 

## REFERENCES

1. Simonsen, N., P. van't Veer, J. J. Strain, J. M. Martin-Moreno, J. K. Huttunen, J. F. Navajas, B. C. Martin, M. Thamm, A. F. Kardinaal, F. J. Kok, et al. 1998. Adipose tissue omega-3 and omega-6 fatty acid content and breast cancer in the EURAMIC study. European Community Multicenter Study on Antioxidants, Myocardial Infarction, and Breast Cancer. *Am. J. Epidemiol.* **147**: 342–352.
2. Shannon, J., I. B. King, R. Moshofsky, J. W. Lampe, D. Li Gao, R. M. Ray, and D. B. Thomas. 2007. Erythrocyte fatty acids and breast cancer risk: a case-control study in Shanghai, China. *Am. J. Clin. Nutr.* **85**: 1090–1097.
3. Storlien, L. H., J. A. Higgins, T. C. Thomas, M. A. Brown, H. Q. Wang, X. F. Huang, and P. L. Else. 2000. Diet composition and insulin action in animal models. *Br. J. Nutr.* **83** (Suppl.): 85–90.
4. Manco, M., A. V. Greco, E. Capristo, D. Gniuli, A. De Gaetano, and G. Gasbarrini. 2000. Insulin resistance directly correlates with increased saturated fatty acids in skeletal muscle triglycerides. *Metabolism.* **49**: 220–224.
5. Storlien, L. H., A. B. Jenkins, D. J. Chisholm, W. S. Pascoe, S. Khouri, and E. W. Kraegen. 1991. Influence of dietary fat composition on development of insulin resistance in rats. Relationship to muscle triglyceride and omega-3 fatty acids in muscle phospholipid. *Diabetes.* **40**: 280–289.
6. Meyer, K. A., L. H. Kushi, D. R. Jacobs, Jr., and A. R. Folsom. 2001. Dietary fat and incidence of type 2 diabetes in older Iowa women. *Diabetes Care.* **24**: 1528–1535.
7. Hu, F. B., and W. C. Willett. 2002. Optimal diets for prevention of coronary heart disease. *J. Am. Med. Assoc.* **288**: 2569–2578.
8. Zancanaro, C., R. Nano, C. Marchioro, A. Sbarbati, A. Boicelli, and F. Osculati. 1994. Magnetic resonance spectroscopy investigations of brown adipose tissue and isolated brown adipocytes. *J. Lipid Res.* **35**: 2191–2199.
9. Miyake, Y., K. Yokomizo, and N. Matsuzaki. 1998. Determination of unsaturated fatty acid composition by high-resolution nuclear magnetic resonance spectroscopy. *J. Am. Oil Chem. Soc.* **75**: 1091–1094.
10. Guillen, M. D., and A. Ruiz. 2003.  $^1\text{H}$  nuclear magnetic resonance as a fast tool for determining the composition of acyl chains in acyl-glycerol mixtures. *Eur. J. Lipid Sci. Technol.* **105**: 502–507.
11. Knothe, G., and J. A. Kenar. 2004. Determination of the fatty acid profile by  $^1\text{H}$ -NMR spectroscopy. *Eur. J. Lipid Sci. Technol.* **106**: 88–96.
12. Yeung, D. K. W., S. L. Lam, J. F. Griffith, A. B. W. Chan, Z. Chen, P. H. Tsang, and P. C. Leung. 2008. Analysis of bone marrow fatty acid composition using high-resolution proton NMR spectroscopy. *Chem. Phys. Lipids.* **151**: 103–109.
13. Lunati, E., P. Farace, E. Nicolato, C. Righetti, P. Marzola, A. Sbarbati, and F. Osculati. 2001. Polyunsaturated fatty acids mapping by  $^1\text{H}$  MR-chemical shift imaging. *Magn. Reson. Med.* **46**: 879–883.
14. Velan, S. S., C. Durst, S. K. Lemieux, R. R. Raylman, R. Sridhar, R. G. Spencer, G. R. Hobbs, and M. A. Thomas. 2007. Investigation of muscle lipid metabolism by localized one- and two-dimensional MRS techniques using a clinical 3T MRI/MRS scanner. *J. Magn. Reson. Imaging.* **25**: 192–199.
15. Beckmann, N., J. J. Brocard, U. Keller, and J. Seelig. 1992. Relationship between the degree of unsaturation of dietary fatty acids and adipose tissue fatty acids assessed by natural-abundance  $^{13}\text{C}$  magnetic resonance spectroscopy in man. *Magn. Reson. Med.* **27**: 97–106.
16. Dimand, R. J., C. T. Moonen, S. C. Chu, E. M. Bradbury, G. Kurland, and K. L. Cox. 1988. Adipose tissue abnormalities in cystic fibrosis: noninvasive determination of mono- and polyunsaturated fatty acids by carbon-13 topical magnetic resonance spectroscopy. *Pediatr. Res.* **24**: 243–246.
17. Moonen, C. T., R. J. Dimand, and K. L. Cox. 1988. The noninvasive determination of linoleic acid content of human adipose tissue by natural abundance carbon-13 nuclear magnetic resonance. *Magn. Reson. Med.* **6**: 140–157.
18. Thomas, E. L., G. Frost, M. L. Barnard, D. J. Bryant, S. D. Taylor-Robinson, J. Simbrunner, G. A. Coutts, M. Burl, S. R. Bloom, K. D. Sales, et al. 1996. An in vivo  $^{13}\text{C}$  magnetic resonance spectroscopic study of the relationship between diet and adipose tissue composition. *Lipids.* **31**: 145–151.
19. Hwang, J. H., S. Bluml, A. Leaf, and B. D. Ross. 2003. In vivo characterization of fatty acids in human adipose tissue using natural abundance  $^1\text{H}$  decoupled  $^{13}\text{C}$  MRS at 1.5 T: clinical applications to dietary therapy. *NMR Biomed.* **16**: 160–167.
20. Strobel, K., J. van den Hoff, and J. Pietzsch. 2008. Localized proton magnetic resonance spectroscopy of lipids in adipose tissue at high spatial resolution in mice in vivo. *J. Lipid Res.* **49**: 473–480.
21. Lund, P., D. Abadi, and J. Mathies. 1962. Lipid composition of normal human bone marrow as determined by column chromatography. *J. Lipid Res.* **3**: 95–98.
22. Field, C. J., A. Angel, and M. T. Clandinin. 1985. Relationship of diet to the fatty acid composition of human adipose tissue structural and stored lipids. *Am. J. Clin. Nutr.* **42**: 1206–1220.
23. Malcom, G. T., A. K. Bhattacharyya, M. Velez-Duran, M. A. Guzman, M. C. Oalman, and J. P. Strong. 1989. Fatty acid composition of adipose tissue in humans: differences between subcutaneous sites. *Am. J. Clin. Nutr.* **50**: 288–291.
24. Beynen, A. C., R. J. Hermus, and J. G. Hautvast. 1980. A mathematical relationship between the fatty acid composition of the diet and that of the adipose tissue in man. *Am. J. Clin. Nutr.* **33**: 81–85.
25. Moriya, K., and S. Itoh. 1969. Regional and seasonal differences in the fatty acid composition of human subcutaneous fat. *Int. J. Biometeorol.* **13**: 141–146.
26. Weis, J., L. Johansson, F. Ortiz-Nieto, and H. Ahlström. 2008. Assessment of lipids in skeletal muscle by high-resolution spectroscopic imaging using fat as the internal standard: Comparison with water referenced spectroscopy. *Magn. Reson. Med.* **59**: 1259–1265.
27. Goodpaster, B. H., and D. Wolf. 2004. Skeletal muscle lipid accumulation in obesity, insulin resistance, and type 2 diabetes. *Pediatr. Diabetes.* **5**: 219–226.